Identifying maximal rigid components in bearing-based localization

Ryan Kennedy, Kostas Daniilidis, Oleg Naroditsky and Camillo J. Taylor

***Abstract*— We present an approach for sensor network localization when provided with a set of angular constraints. This problem arises in camera networks when angles between nearby points can be measured but depth measurements are not readily available. We provide contributions for two different variations on this problem. First, when each node is aware of a global coordinate frame, we present a novel method for identifying the components of the problem that are rigidly constrained. Second, in the more difficult case where only relative angles are known, we propose a novel spectral solution that achieves a globally-optimal embedding under transitively-triangular constraints, which we show encompass a wide range of real-world conditions. We demonstrate the utility of our algorithm on both synthetic data and data from quadrotor robot formations.**

I. INTRODUCTION

Self-localization of camera networks is a problem that arises whenever cameras are deployed in a static configuration or are mounted on robots. Monocular cameras can measure line of sight to the other cameras but are not able to easily determine distances. Finding the space of possible camera positions that are consistent with these measurements is a variant of the bearing-based or angle-of-arrival sensor network localization problem. Note that this problem differs from multi-robot localization and mapping where robots can sense other points in the environment.

We address this problem for two different cases: when orientation with respect to a global reference frame is given (for instance, when each agent has a compass), and when only relative bearing measurements are available. In both cases we focus on static data. Global rigidity has been previously studied when global orientation is known [1], [2] and the case of relative bearings has been studied with respect to its computational complexity [3].

Due to occlusion and other visibility conditions, it is rarely the case that a camera network is globally-rigid with respect to the set of measurements and so a solution is needed for identifying rigid components. Such components can be used to establish a local reference frame and enable target tracking, 3D triangulation, and any other 3D guidance and control of an agent visible to the cameras of this component.

In this paper we present the following contributions to bearing-based localization:

1) For the case of known absolute heading we present a linear algebraic solution for the identification of rigid components based on the null space of the global rigidity problem. This result holds for any dimension of the underlying Euclidean space.
2) For the case of only relative bearing measurements in 2D, we introduce a new approach for the identification of a subset of all rigid components, which is based on a recursive definition of rigidity starting from triangles. We also present a novel solution for the embedding problem under such constraints without fixing two points as a reference for reconstruction. We make use of its generality to solve the embedding problem for any triangulated network even in the presence of noise, giving a globally-optimal embedding in seconds even for very large networks.

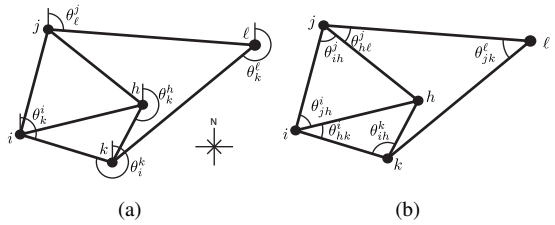

Fig. 1: **(a)** A directed network of nodes with global angle measurements; when a global orientation reference is available, angles can be measured with respect to this coordinate system. **(b)** A directed network of nodes with relative angle measurements. The component formed by nodes h, i, j and k is a rigid set of triangular constraints while node ℓ is connected rigidly to this component.

The literature on sensor network localization is overwhelming. Most of the approaches assume known position of some anchor nodes and *distance* measurements. The corresponding theory on uniqueness of localization and its complexity are comprehensively treated in [4]. The anchor-free relative measurement problem formulation is based on relative distance measurements and is related to the well known problems of graph rigidity [5], [6], multi-dimensional scaling [7], and parallel mechanisms [8]. One of the most complete treatments for the anchor-based and anchor-free case can be found in [4]. From this analysis we would like to note the trilateration result (also in [9]) which is related to our triangle construction: if a graph in dimension d has a complete subgraph with $d+1$ nodes and the rest of the nodes can be incrementally added by connecting with the previous graph, then the graph is uniquely localizable and can be realized in polynomial-time. In [10] the result is extended to show that any uniquely localizable graph can be realized

Support by the ARL Robotics Collaborative Technology Alliance ARL RCTA W911NF-10-2-0016 is gratefully acknowledged.

Authors are with the GRASP Lab, Department of Computer and Information Science, University of Pennsylvania. kenry@cis.upenn.edu

in polynomial time via semidefinite programming. The noisy distance measurement case has been treated in [11], [12], [13] among many others.

Let us switch to the case of bearing measurements – also known as angle-of-arrival measurements – where we differentiate between approaches with measured absolute bearings (Section III) and relative bearings (Section IV). The case of a given global reference frame as studied in Section III is also known as *parallel drawing* and its realization has been studied in [1], [2] using the same orthogonality constraint that we use. The rank conditions for the homogeneous case are proved in [1] but no solution is given for the identification of rigid components in the underdetermined so-called *flexible* parallel drawing case. In the noisy bearing case an approach [14] for localization based on bounded uncertainty of relative bearings was proposed and solved approximately using linear programming.

There are very few results when only relative bearings are available and these are usually related to moving formations [15], [16]. The general 2D case where bearing measurements between nodes are not mutual (i.e., two nodes see cannot each other) has been proven NP-hard in [3]. A footnote in [3] hints that in the case where relative measurements are mutual, localization can be achieved in polynomial time. A related approach using relative bearing measurements between cameras and landmarks in 2D was given by [17], but their method deals with only three views at a time and first determines camera pose [18] before subsequently finding landmark locations. In contrast, here we make no distinction between cameras and landmarks and consider all constraints simultaneously. A characterization of rigidity for certain classes of relative angle constraint systems was also explored in [22].

Regarding relative measurements in 3D, the most complete treatment can be found in [19] where more than one time-point of a 3D formation is considered due to the general static 3D case being underdetermined. We will not refer here to the plethora of papers on formation control which relate to estimation based approaches for localization of robot teams over time.

We believe that our result is the first to provide linear constraints for efficient localization in the case of relative bearing measurements. We also offer a concrete algorithm for identifying rigid components in the absolute bearing case.

II. PROBLEM DESCRIPTION

Given a sensor network consisting of n nodes, we consider two problems where nodes can measure the bearing to a subset of others. In the first case, measurements are done with respect to a *global* coordinate system where each node i can measure the bearing $\theta_j^i \in [0, 2\pi]$ between a global orientation and another node j (Figure 1a). In the second case, only *local* orientation measurements are available, so a node i can measure the relative bearing $\theta_{jk}^i \in [0, 2\pi]$ from node j to k within its sensor range (Figure 1b). In both cases our goal is to compute the possible spatial configurations of the sensor network.

In the global case, we represent the problem as a graph $G = (\mathcal{E}, \mathcal{V})$ consisting of n vertices and m directed edges where each angle measurement θ_j^i is the bearing of node j with respect to node i. The goal of the the graph embedding problem is to find an embedding that assigns to each vertex $i \in \mathcal{V}$ a d-dimensional point $\mathbf{x}_i \in \mathbb{R}^d$ such that all angle constraints are satisfied. In this paper we focus on $d = 2$ or 3.

For an embedding problem in $\mathbb{R}^d$, we write the location of node i as $\mathbf{x}_i = \begin{bmatrix} x_i^1 & \dots & x_i^d \end{bmatrix}$. Given an embedding $\mathbf{x} = \begin{bmatrix} \mathbf{x}_1 & \dots & \mathbf{x}_n \end{bmatrix}^T \in \mathbb{R}^{dn}$ satisfying all angular constraints, any translation or scaling of $\mathbf{x}$ is also a valid embedding since these transformations maintain the global angles between nodes. Additionally, when no global coordinate system is known, embeddings are also invariant to arbitrary rotations. If a single, unique solution $\mathbf{x}$ exists for an embedding problem (up to these invariant transformations), we say that this solution is *rigid*. Furthermore, if any subset of vertices $V \subset \mathcal{V}$ is sufficiently constrained such that a single, unique solution exists for the embedding problem when restricted to V, we say that V forms a *rigid subproblem*.

III. GLOBAL ANGLE MEASUREMENTS

We first consider the embedding problem in $\mathbb{R}^3$ when a global orientation reference is known to all nodes (Figure 1a). Let θ_j^i be the angle that node i measures between a global reference direction and another node j and let $\mathbf{d}_{ij}$ be a unit vector pointing in this direction. For an embedding $\mathbf{x} \in \mathbb{R}^{3n}$ to be consistent with this constraint, $\mathbf{d}_{ij}$ and $(\mathbf{x}_j - \mathbf{x}_i)$ should be parallel. Equivalently, their cross product must be zero:

$$\mathbf{d}_{ij} \times (\mathbf{x}_j - \mathbf{x}_i) = \mathbf{0}. \tag{1}$$

This cross product constraint can be written in matrix form as

$$\mathbf{d}_{ij} \times (\mathbf{x}_j - \mathbf{x}_i) = \begin{bmatrix} 0 & -d_{ij}^3 & d_{ij}^2 \\ d_{ij}^3 & 0 & -d_{ij}^1 \\ -d_{ij}^2 & d_{ij}^1 & 0 \end{bmatrix} \begin{bmatrix} x_j^1 - x_i^1 \\ x_j^2 - x_i^2 \\ x_j^3 - x_i^3. \end{bmatrix} = \begin{bmatrix} 0 \\ 0 \\ 0 \end{bmatrix} \tag{2}$$

and thus each measured $\mathbf{d}_{ij}$ provides a set of three linear constraints (two of which are linearly independent) on $\mathbf{x}$. The entire set of $3m$ linear constraints can be stacked to form a matrix $\mathbf{A}$, resulting in the homogeneous linear system

$$\mathbf{A}\mathbf{x} = \mathbf{0}. \tag{3}$$

Any $\mathbf{x} \in \mathbb{R}^{3n}$ satisfying Equation (3) is a valid embedding for the given directional constraints. This linear system can be solved by finding the null space of the $3m \times 3n$ matrix $\mathbf{A}$. However, in the presence of noise, the constraints might not be satisfiable. In this case, the eigenspace corresponding to a set of the smallest eigenvectors of $\mathbf{A}$ will give an approximate solution.

A related spectral solution is given by Brand [20], who constructs a symmetric matrix $\mathbf{H}_\mathcal{E}$ and their solution to the embedding problem is given by the vector space that is spanned by the eigenvectors of $\mathbf{H}_\mathcal{E}$ corresponding to eigenvalues equal to 0. The connection between their formation and ours is given in the following theorem.

Theorem 1: The matrix $\mathbf{H}_{\mathcal{E}}$ given by Brand [20] is related to our constraint matrix $\mathbf{A}$ by $\mathbf{H}_{\mathcal{E}} = \mathbf{A^T A}$. Furthermore, the corresponding solutions are the same.

Proof: Let $\mathbf{v}_{ij} = (\mathbf{x}_j - \mathbf{x}_i)$ and define an error function as

$$\mathcal{E}_{ij} = ||\mathbf{d}_{ij} \times \mathbf{v}_{ij}||_2^2, \tag{4}$$

which measures the deviation that $\mathbf{d}_{ij}$ and $\mathbf{v}_{ij}$ are from being parallel. Using the relationship between cross products and dot products, this is equivalent to

$$\begin{aligned} \mathcal{E}_{ij} &= ||\mathbf{d}_{ij}||_2^2 \cdot ||\mathbf{v}_{ij}||_2^2 - (\mathbf{d}_{ij} \cdot \mathbf{v}_{ij})^2 && (5) \\ &= \mathbf{d}_{ij}^T \mathbf{d}_{ij} \mathbf{v}_{ij}^T \mathbf{v}_{ij} - \mathbf{v}_{ij}^T \mathbf{d}_{ij} \mathbf{d}_{ij}^T \mathbf{v}_{ij} && (6) \end{aligned}$$

This can be written in matrix form as

$$\mathcal{E}_{ij} = \mathbf{v}_{ij}^T \left[\mathbf{d}_{ij}^T \mathbf{d}_{ij} \mathbf{I} - \mathbf{d}_{ij} \mathbf{d}_{ij}^T \right] \mathbf{v}_{ij} \tag{7}$$

The internal matrix $\mathbf{d}_{ij}^T \mathbf{d}_{ij} \mathbf{I} - \mathbf{d}_{ij} \mathbf{d}_{ij}^T$ is exactly the term given in Equation (4) of Brand [20], and therefore the cost function given by Equation (3) in their paper is identical to our cost function $\mathcal{E}_{ij}$ (in three dimensions). Since the matrix $\mathbf{A}$ in Equation (3) is a stack of linear constraints of the form $\mathbf{d}_{ij} \times (\mathbf{x}_j - \mathbf{x}_i) = \mathbf{0}$, then if we write $\mathbf{x}^T (\mathbf{A}^T \mathbf{A}) \mathbf{x} = 0$, this requires that $||\mathbf{d}_{ij} \times (\mathbf{x}_j - \mathbf{x}_i)||_2^2 = 0$. Since $\mathbf{A}^T \mathbf{A}$ is clearly positive semidefinite, we can minimize the cost function $\mathcal{E}_{ij}$ by taking the minimum eigenvectors of $\mathbf{A}^T \mathbf{A}$, but since this is the same as Brand's cost function, the corresponding matrices must be the same and we have $\mathbf{H}_{\mathcal{E}} = \mathbf{A}^T \mathbf{A}$.

Next we show that the solutions to the two problems are identical. A basis for the null space of $\mathbf{A}$ is given by the set of right singular vectors with vanishing singular values. Let $\mathbf{A} = \mathbf{U \Sigma V}^T$ be a singular value decomposition of $\mathbf{A}$. Then $\mathbf{H}_{\mathcal{E}}$ is given by

$$\mathbf{H}_{\mathcal{E}} = \mathbf{V \Sigma}^2 \mathbf{V}^T. \tag{8}$$

Thus, the eigenvectors of $\mathbf{H}_{\mathcal{E}}$ which have an eigenvalue of 0 are exactly the singular vectors of $\mathbf{A}$ which have a singular value of 0. ∎

We have therefore given a different characterization of the problem presented by Brand which has the slight advantage of having simpler notation.

Ideally, the set of constraints will be sufficient to have a rigid solution. The null space of a rigid solution will have dimension 4, corresponding to one embedding and the embeddings produced by scaling, or translating along each of the x, y and z axes. However, it is also possible that the problem constraints may be degenerate. This can occur either because there are multiple connected components in the connectivity graph or because all constraints on a node are collinear. By investigating the properties of a basis that spans the null space of $\mathbf{A}$, we are able to navigate through the space of solutions that satisfy all the problem constraints.

Let

$$\mathbf{N} = \begin{bmatrix} | & & | \\ \mathbf{c}_1 & \dots & \mathbf{c}_k \\ | & & | \end{bmatrix} \tag{9}$$

be a matrix whose columns span the k-dimensional null space of $\mathbf{A}$. Since $\mathbf{A}\mathbf{c}_i = \mathbf{0}$ for all $\mathbf{c}_i$, then any linear combination of the columns of $\mathbf{N}$ will also lie in the null space of $\mathbf{A}$. More formally, we have

$$\mathbf{Ax} = \mathbf{0}, \tag{10}$$

where

$$\mathbf{x} = \mathbf{Nw} \tag{11}$$

for any $\mathbf{w} \in \mathbb{R}^k$. By varying $\mathbf{w}$, any solution consistent with the problem constraints can be realized.

A. Identifying Rigid Components

When an embedding problem does not admit a rigid solution, we can instead locate subsets of vertices $V \subset \mathcal{V}$ and the associated edges $E_V = \{(i,j) \in \mathcal{E} \mid i,j \in V\}$ and constraints $D_V = \{\mathbf{d}_{ij} \in \mathcal{D} \mid i,j \in V\}$ such that the embedding problem when restricted to this subproblem does have a rigid solution.

Trivially, the sets consisting of only pairs of nodes are rigidly constrained since scaling and translation of both points together are the only possible transformations that can be done. However, it would be more useful to find the *maximal* rigid subproblems.

Theorem 2: The set of edges of all maximal rigid subproblems $\mathcal{M} = \{E_V\}$ induce a *partition* of the original edge set $\mathcal{E}$. That is, each edge $e \in \mathcal{E}$ is included in exactly one maximal rigid subproblem edge set $E_V \in \mathcal{M}$.

Proof: Since each edge is in the rigid subproblem consisting of just itself, each edge must be in at least one rigid subproblem. Suppose that it were in two maximal rigid subproblems. Since they are both maximal, each can be scaled independently, but an edge can only have one length and so this gives a contradiction. Therefore, each edge is part of exactly one maximal subproblem. ∎

Let $\mathbf{x}$ be a solution to an embedding problem. Because any translation of $\mathbf{x}$ in space is also a valid solution, suppose that we translate the embedding such that $\mathbf{x}_i = \mathbf{0}$ and node i is identified with the origin. We now show how the maximal fully constrained subproblems associated with node i can be found. By repeating this process for each node, all such subproblems can be determined.

Let $\mathbf{r}_i$ be the i^{th} set of 3 rows of $\mathbf{N}$, corresponding to the three dimensions of the position of node i over all basis vectors of the null space so that

$$\mathbf{N} = \begin{bmatrix} - & \mathbf{r}_1^T & - \\ & \vdots & \\ - & \mathbf{r}_n^T & - \end{bmatrix}. \tag{12}$$

We fix node i to be embedded to the origin by setting $\mathbf{x}_i = \mathbf{0}$. Since $\mathbf{x}_i^T = \mathbf{r}_i^T \mathbf{w}$, we subtract $\mathbf{x}_i^T$ from each set of rows in the left-hand side and $\mathbf{r}_i^T \mathbf{w}$ from each set of rows on the right-hand side of Equation (11) . The resulting constraint has $\mathbf{x}_i = \mathbf{0}$. Define this modified null space matrix as

$$\mathbf{N}^{(i)} = \begin{bmatrix} \mathbf{r}_1^T - \mathbf{r}_i^T \\ \vdots \\ \mathbf{0} \\ \vdots \\ \mathbf{r}_n^T - \mathbf{r}_i^T \end{bmatrix}. \tag{13}$$

This gives us a new equation,

$$\mathbf{x} = \mathbf{N}^{(i)}\mathbf{w}, \tag{14}$$

where a given value of $\mathbf{w} \in \mathbb{R}^k$ will yield an embedding $\mathbf{x}$ such that $\mathbf{x}_i$ is at the origin. We have eliminated some freedom of translation by requiring that $\mathbf{x}_i$ be embedded to the origin. In particular, given a maximal fully constrained subproblem that contains the node i, any edge in this subproblem can only be scaled and not translated (or else either $\mathbf{x}_i$ would not be at the origin or it would not be a rigid subproblem), and so all pairs of edge lengths within fully constrained subproblems containing node i will have constant ratios. Furthermore, because we have translated node i to the origin, these edge lengths are simply their distances from the origin up to scale. This brings us to the following theorem.

Theorem 3: Nodes j and k with $j, k \neq i$ are a part of a maximal rigid component with node i if and only if the three rows of $\mathbf{N}^{(i)}$ corresponding to node j are parallel with the corresponding rows for node k.

Proof: Suppose that j and k are in the same rigid component as i. Since the rigid subproblem can only be scaled without violating constraints (since i is fixed to the origin), then for any given embedding, the ratio $||\mathbf{x}_j||_2^2/||\mathbf{x}_k||_2^2$ is constant. Equivalently,

$$\frac{\left[\mathbf{N}^{(i)}\mathbf{w}\right]_j}{\left[\mathbf{N}^{(i)}\mathbf{w}\right]_k} = \alpha \quad \forall\ \mathbf{w} \in \mathbb{R}^k \tag{15}$$

for some constant α, where the j^{th} and k^{th} rows can be any of the three corresponding rows for node j and k (The constant α may be different for each of the three pairs of rows since the ratios between the x, y and z coordinates may be different.). *This can occur only if the j^{th} and k^{th} rows of $\mathbf{N}^{(i)}$ are parallel.*

Conversely, suppose that the rows are parallel. Then the ratio given in Equation (15) is constant and therefore the ratio $||\mathbf{x}_j||_2^2/||\mathbf{x}_k||_2^2$ is constant. This implies that only scaling can occur and so j and k are in the same rigid component as i, or else it would be possible to translate them.

■

For any two nodes j and k in the same rigid component as i, all three rows of i must be parallel with all three rows of j. This can be measured by taking the maximum cosine distance between two nodes over all three of their corresponding rows. All maximal fully constrained subproblems of node i can thereby be found by identifying sets of parallel rows of the matrix $\mathbf{N}^{(i)}$, and the corresponding edge set and associated directional constraints will form a maximal rigid subproblem. By repeating this process for each node, all fully constrained subproblems can be identified.

The complexity of this algorithm is dominated by the computation of rigid components, especially since $\mathbf{A}$ is sparse. To identify rigid components, a cosine distance matrix must be computed for each node i. This can be done in $O(kn^2)$ time, where k is the dimensionality of the null space, for a total cost of $O(kn^3)$. However, the multiplicative constant here is small and it can easily be parallelized for large problems since the computation of each node can be done independently. We found that for a random network of under 200 nodes of degree 3 the entire algorithm took less than a second, while for 500 nodes the null space could be calculated in around a second and the rigid components could be found in 14 seconds on a standard laptop computer.

IV. RELATIVE ANGLE MEASUREMENTS

We now proceed to the more difficult case when no global coordinate frame exists and nodes are only able to measure relative angles between other nodes. We restrict the problem to $\mathbb{R}^2$ where we can derive quadratic constraints based on the given angle measurements (the extension to $\mathbb{R}^3$ is not trivial). An embedding of nodes in the plane is then given by $\mathbf{x} \in \mathbb{R}^{2n}$.

Let θ_{jk}^i be the measured angle between nodes j and k from the perspective of node i (Figure 1b). We desire an embedding such that the angle between $(\mathbf{x}_j - \mathbf{x}_i)$ and $(\mathbf{x}_k - \mathbf{x}_i)$ is θ_{jk}^i. In such an embedding, rotating the vector $(\mathbf{x}_j - \mathbf{x}_i)$ by θ_{jk}^i would result in parallel vectors and a further rotation by $\pi/2$ would result in the two vectors being perpendicular. Let $\mathbf{R}_\theta$ be a 2×2 rotation matrix by the angle θ. Then, the two vectors $(\mathbf{x}_k - \mathbf{x}_i)$ and $\mathbf{R}_{\theta_{jk}^i + \frac{\pi}{2}}(\mathbf{x}_j - \mathbf{x}_i)$ will be perpendicular in an embedding that satisfies the constraint and so their inner product will vanish:

$$(\mathbf{x}_k - \mathbf{x}_i)^T \mathbf{R}_{\theta_{jk}^i + \frac{\pi}{2}} (\mathbf{x}_j - \mathbf{x}_i) = 0. \tag{16}$$

This is the same constraint that was derived by Taylor and Spletzer [21]. The constraint is quadratic with respect to $\mathbf{x}$ and has the equivalent matrix form

$$\begin{bmatrix}\mathbf{x}_i & \mathbf{x}_j & \mathbf{x}_k\end{bmatrix} \mathbf{M}_{jk}^i \begin{bmatrix}\mathbf{x}_i \\ \mathbf{x}_j \\ \mathbf{x}_k\end{bmatrix} = \mathbf{0}, \tag{17}$$

where

$$\mathbf{M}_{jk}^i = \begin{bmatrix} \mathbf{R}_{\theta_{jk}^i + \frac{\pi}{2}} + \mathbf{R}_{\theta_{jk}^i + \frac{\pi}{2}}^T & -\mathbf{R}_{\theta_{jk}^i + \frac{\pi}{2}} & -\mathbf{R}_{\theta_{jk}^i + \frac{\pi}{2}}^T \\ -\mathbf{R}_{\theta_{jk}^i + \frac{\pi}{2}}^T & \mathbf{0} & \mathbf{R}_{\theta_{jk}^i + \frac{\pi}{2}}^T \\ -\mathbf{R}_{\theta_{jk}^i + \frac{\pi}{2}} & \mathbf{R}_{\theta_{jk}^i + \frac{\pi}{2}} & \mathbf{0} \end{bmatrix}. \tag{18}$$

Although this is written only in terms of $\mathbf{x}_i$, $\mathbf{x}_j$ and $\mathbf{x}_k$, it can be expanded into a full $2n \times 2n$ matrix by filling in the appropriate matrix elements, giving

$$\mathbf{x}^T \mathbf{M}_{jk}^i \mathbf{x} = \mathbf{0}. \tag{19}$$

Each pairwise angle measurement provides one such quadratic constraint and so a configuration of multiple nodes yields a set of measurements $\mathcal{M} = \{\mathbf{M}_i\}_{i \in \{1,\ldots,m\}}$. An embedding $\mathbf{x} \in \mathbb{R}^{2n}$ will satisfy all constraints exactly when

$$\mathbf{x}^T \mathbf{M}_i \mathbf{x} = 0 \quad \forall\ \mathbf{M}_i \in \mathcal{M}. \tag{20}$$

The set of all solutions to Equation (20) is straightforward to calculate if all $\mathbf{M}_i$ are positive semidefinite matrices, as the following theorem shows.

Theorem 4: Given a set of constraints

$$\mathbf{x}^T \mathbf{A}_1 \mathbf{x} = 0, \ldots, \mathbf{x}^T \mathbf{A}_m \mathbf{x} = 0, \tag{21}$$

with all matrices symmetric positive semidefinite ($\mathbf{A}_i \succeq \mathbf{0}$), a vector $\mathbf{x}$ satisfies all constraints if and only if it is in the null space of the combined matrix $\hat{\mathbf{A}} = \mathbf{A}_1 + \cdots + \mathbf{A}_m$.

Proof: In the forward direction, if $\mathbf{x}^T\mathbf{A}_i\mathbf{x} = 0$ holds for all $i \in \{1 \dots m\}$, then

$$\mathbf{x}^T\hat{\mathbf{A}}\mathbf{x} = \mathbf{x}^T\mathbf{A}_1\mathbf{x} + \cdots + \mathbf{x}^T\mathbf{A}_m\mathbf{x} = 0. \tag{22}$$

and thus $\mathbf{x}$ is in the null space of $\hat{\mathbf{A}}$.

Conversely, if $\mathbf{x}$ is in the null space of $\hat{\mathbf{A}}$, then Equation (22) holds. Since each $\mathbf{A}_i$ is positive semidefinite, we must have $\mathbf{x}^T\mathbf{A}_i\mathbf{x} \geq 0$ for all i. The sum of non-negative real numbers can be zero only when each individual term is zero, and therefore $\mathbf{x}^T\mathbf{A}_i\mathbf{x} = 0$ for all i. ∎

This tells us that if $\mathbf{M}_i \succeq \mathbf{0}$ for all i, then the solution space is given simply by the null space of the the sum of all of the constraint matrices. Unfortunately, $\mathbf{M}_i$ are generally not positive semidefinite, as was also noted by Taylor [21].

A. Triangle Constraints

Consider the case of a *triangle*, where each node i, j and k is aware of the other two and $\theta^i_{jk} + \theta^j_{ik} + \theta^k_{ij} = \pi$. In the following, we let $\theta_i = \theta^i_{jk}$ when there is no ambiguity. Let $\mathbf{M}_i$, $\mathbf{M}_j$ and $\mathbf{M}_k$ be the three constraint matrices associated with θ_i, θ_j and θ_k, respectively. Although each $\mathbf{M}_i$ is not positive semidefinite on its own, they can be combined to form a positive semidefinite constraint that exactly captures the combination of the three constraints. This brings us to our main result when no global orientation is known.

Theorem 5: Let i, j and k be three nodes, each of which can see the other two and let θ_i, θ_j and θ_k be the associated angle measures such that $\theta_i + \theta_j + \theta_k = \pi$. If $\mathbf{M}_i, \mathbf{M}_j$ and $\mathbf{M}_k$ are the corresponding constraint matrices as defined in Equation (18), then the matrix

$$\mathbf{M} = \sin\theta_i\mathbf{M}_i + \sin\theta_j\mathbf{M}_j + \sin\theta_k\mathbf{M}_k \tag{23}$$

is positive semidefinite. Furthermore, a vector $\mathbf{x}$ will satisfy $\mathbf{x}^T\mathbf{M}\mathbf{x} = 0$ if and only if $\mathbf{x}$ corresponds to a triangle with angles equal to θ_i, θ_j and θ_k.

Proof: Using the fact that the angles of a triangle sum to π radians, there are two non-zero eigenvalues[1] of the matrix $\mathbf{M}$, both of which are equal to

$$3 - \cos(2\theta_i) - \cos(2\theta_j) - \cos(2\theta_i - 2\theta_j). \tag{24}$$

Since the cosine function is always ≤ 1 the eigenvalues are always non-negative, and therefore $\mathbf{M} \succeq \mathbf{0}$.

Now, let $\mathbf{x}$ be an embedding and let γ_i, γ_j and γ_k be the angles between node i, j and k in the embedding. We want to show that it must be that $\gamma_i = \theta_i$, $\gamma_j = \theta_j$ and $\gamma_k = \theta_k$. The reason for this comes from the fact that $\mathbf{M}$ has a null space of dimension 4. Given any embedding $\mathbf{x}$ that satisfies $\mathbf{x}^T\mathbf{M}\mathbf{x} = 0$, we can rotate, translate and scale the embedding without violating this constraint since $\mathbf{M}$ was defined only in terms of relative angles of the triangle. This implies that the solution set corresponding to the null space of $\mathbf{M}$ is a set of rigid embeddings. However, we know that the triangle with angles θ_i, θ_j and θ_k satisfies $\mathbf{x}^T\mathbf{M}\mathbf{x} = 0$, and therefore any triangle must have the same angles or else $\mathbf{M}$ would have a larger null space corresponding to additional degrees of freedom. ∎

Theorem 5 provides us with a quadratic constraint that exactly characterizes triangles in the plane. Furthermore, this constraint is positive semidefinite. This has an important consequence: if our set of constraints consists entirely of triangles, we can find the entire solution space of embeddings which satisfy all constraints simultaneously by finding the null space of the combined constraint matrix.

B. Transitive Triangle Constraints

Using this method, we are able to solve the embedding problem when all constraints are triangular. The solutions that we obtain consist of rigid components where each rigid component is a set of edge-adjacent triangles. The reason that this is rigid follows from the fact that any triangle with two angles measured is rigid, as is shown in the following lemma.

Lemma 1: A triangular set of three nodes $i, j, k \in \mathcal{V}$ is rigid if any two of the associated angles θ_i, θ_j or θ_k are measured.

Proof: Because the angles of a triangle must sum to π, any two measured angles are sufficient to calculate the third. The law of sines tells us that

$$\frac{a}{b} = \frac{\sin A}{\sin B} \tag{25}$$

for any two side lengths a and b and opposite angles A and B of the triangle. Since the angles of this triangle are all defined, the ratio of the side lengths must remain constant and therefore the triangle is rigid. ∎

Because a triangle is rigid, in the noise-free case it is possible to pick a reference edge of a triangle and reconstruct the third point based on the given angle measurements. However, in the case of multiple edge-connected triangles, it would be beneficial to not have to define such a reference; Theorem 5 says that we do not need to since each triangle has a positive semidefinite constraint that characterizes it. Also, using the optimization based by Theorem 5 allows us to naturally handle noise (Section IV-C).

Although triangles occur frequently in real-world data (see Section V), there are rigid embedding problems which do not directly have triangular constraints. One subset of these rigid problems is characterized in the following lemma.

Lemma 2: Let $V \subset \mathcal{V}$ be a rigid subproblem, and let $w \notin V$ be another node. If w measures an angle θ^w_{ij} between two nodes $i, j \in V$, and if additionally either i measures an angle θ^i_{kw} or j measures an angle θ^j_{kw} for $k \in V$, then the subproblem defined by $V \cup \{w\}$ is rigid.

Proof: Because V is a rigid component, the angles θ^i_{jk} for any $i, j, k \in V$ must remain constant. Thus, even if a given angle θ^i_{jk} is not directly measured by the sensors, its value is implicit in the other constraints and we can consider all such angles to exist. Furthermore, if i measures an angle θ^i_{jw} for $j \in V$ and $w \notin V$, then the angles θ^i_{kw} for $k \in V$ are also implicit since the angles θ^i_{jk} are known.

[1]Eigenvalues were calculated symbolically using Mathematica.

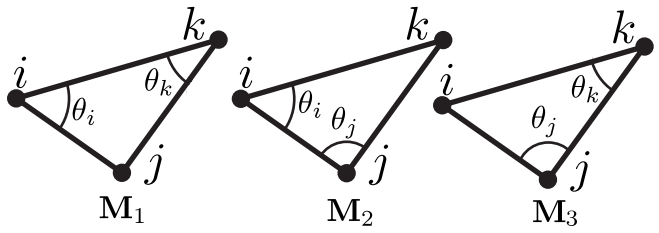

Fig. 2: One constraint matrix is created for each set of two angular measurements on three nodes. In the presence of noise, the three constraints will differ and our method will find a globally-optimal solution with respect to the three constraints.

Suppose that $w \notin V$ measures the angle θ_{ij}^w for $i, j \in V$, and that i also measures θ_{kw}^i for $k \in V$. Because angle θ_{jw}^i is implicitly known, two angles in the triangle consisting of i, j, w are known and by Lemma 1 this triangle is rigid. Because the edge (i, j) is shared by both this triangle and the rigid component V, the entire component $V \cup \{w\}$ is rigid. ■

Although our algorithm deals only with triangles directly, we can extend it to nodes which are transitively and rigidly connected to triangular subproblems using Lemma 2. We know that an edge-connected triangular subproblem is rigid, and thus all internal angles of the subproblem are implicitly defined. This allows us to create new triangular constraints for nodes which are rigidly connected to the subproblem. In this way, we can add triangular constraints to a larger subset of rigid embedding problems.

C. Dealing with Noise

In real-world situations, sensor measurements will have noise and the sum of three angle constraints in any given triangle will not be exactly π, making Theorem 5 invalid. To deal with noise, we view each set of two angular constraints incident on three points as a full triangle. Because each triangle is rigidly defined by just two constraints (Lemma 1), we add a third angle to every set of two so that an exact triangle is formed, as shown in Figure 2.

When three constraints forming a triangle are given as part of the measured data, this results in a set of three overlapping constraint matrices rather than just one. If the measured angles sum to π then all three matrices will be identical, but if there is noise then the matrices will differ. In the case of noise, the exact null space of the combined constraint matrix will be trivial since no non-trivial embedding can simultaneously satisfy all three conflicting constraints. However, the eigenvectors of the combined constraint matrix that correspond to the four smallest eigenvalues will provide an embedding which gives a globally-optimal rigid solution with respect to the cost function based on all of these constraints, as we now show.

Consider a set of triangular constraints formed by the nodes i, j and k (Figure 2). Using the above construction, we create three constraint matrices $\mathbf{M}_1, \mathbf{M}_2$ and $\mathbf{M}_3$, where the

Fig. 3: A formation of quadrotors.

matrices differ due to measurement noise. From Theorem 5, we know that $\mathbf{x}^T\mathbf{M}_i\mathbf{x} = 0$ for a consistent embedding and is strictly positive otherwise. We thus consider each $\mathbf{x}^T\mathbf{M}_i\mathbf{x}$ to be a measure of how much the embedding $\mathbf{x}$ violates the constraint $\mathbf{M}_i$. A globally-optimal embedding is given by solving the optimization problem

$$\min_{\mathbf{x}} \mathbf{x}^T\mathbf{M}_1\mathbf{x} + \mathbf{x}^T\mathbf{M}_2\mathbf{x} + \mathbf{x}^T\mathbf{M}_3\mathbf{x} = \mathbf{x}^T \sum_i \mathbf{M}_i\mathbf{x}. \quad (26)$$

Because each $\mathbf{M}_i$ is positive semidefinite, so is the sum $\sum_i \mathbf{M}_i$. The solution to this problem is given by the eigenvectors of $\sum_i \mathbf{M}_i$ corresponding to the four smallest eigenvalues, since a rigid embedding will have four degrees of freedom (a problem with multiple triangulated components can be easily split into separate rigid components). Thus, by constructing a set of three constraints for each triangle, our method results in a globally-optimal solution in the presence of measurement noise. Also, by weighting each matrix $\mathbf{M}_i$, Equation (26) can be made to give preference to certain constraints, which is useful when the relative accuracy of measurements is known.

Noise also makes extending triangular constraints transitively to other nodes difficult. Without noise, all implicit constraints could be directly calculated. However, if measurements are noisy then it's not clear how to set the angles for implicit constraints. We propose the following approach. First, each rigid triangular component can be embedded using the previously-described method. Given this embedding, all noisy angle measurements within these components are reconciled and all implicit angle constraints can be added without ambiguity. Any node which is rigidly connected to one of these components can then be added to the problem and by calculating a new embedding using these triangular constraints, the attached nodes will be incorporated. This process can be continued iteratively until any node which is transitively connected to a triangular rigid component is added to the embedding.

The complexity of this algorithm can be split into two steps. In the first, all triangle constraints must be identified, which can be done in linear time if each node has a constant degree by seeing whether connections of connections of a node point back to itself. Finding the null space of such a matrix will take $O(n)$ time per iteration using, for example, Lanczos iteration [23].

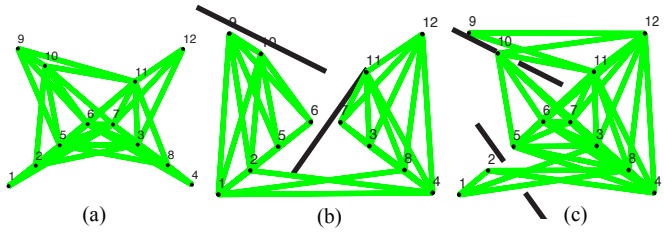

Fig. 4: We generate data according to three visibility models: (a) each node can view others within a fixed radius, (b) randomly-placed walls obstruct visibility, and (c) randomly-placed pairs of pillars to obstruct visibility.

V. EXPERIMENTS

We demonstrate the use of our methods using two types of data. The first consists of entirely synthetic data, where we generate 20 random points in the plane under realistic measurement constraints. In particular we use three different visibility models, as shown in Figure 4:

1) *Local visibility*: each node is able to sense other nodes within a fixed radius.
2) *Walls:* two walls are randomly placed in the plane which obstruct the view between nodes.
3) *Pillars:* two pairs of pillar pairs are randomly placed in the plane.

Second, we use a dataset from [24] based on kQuadNano quadrotors developed by KMel Robotics which have a diameter of 21 cm (see Figure 3). This dataset consists of 12 quadrotors within a 4×4-meter area. Although the angle measurements are also synthetic in this case, the formations are more realistic than simply using random points.

A. Global Angle Measurements

We first consider the case when angle measurements are made with respect to a global coordinate frame. Figure 5 demonstrates how we are able to identify the rigid components of any embedding problem. Although a given solution to an embedding problem may have many degrees of freedom when it is underconstrained, each rigid subproblem will be fixed up to scale and translation.

B. Relative Angle Measurements

We also demonstrate our proposed algorithm for calculating embeddings when only relative angle measurements are available. Quantitative results are shown in Table I for different conditions and various amounts of noise. We use noise that is normally-distributed with $0.1, 0.3$ and 0.5-degree standard deviations in addition to uniform noise between 0 and 1 degree. These noise measures corresponds to errors of $1.67, 5.03, 8.38$ and 16.76 pixels, respectively, in a 1920×1080-pixel resolution HD camera with a 90-degree horizontal field of view. Such an error in a line-of-sight bearing measurement can be induced, for example, by the uncertainty in the measurement of the centroid of the appearance of another robot.

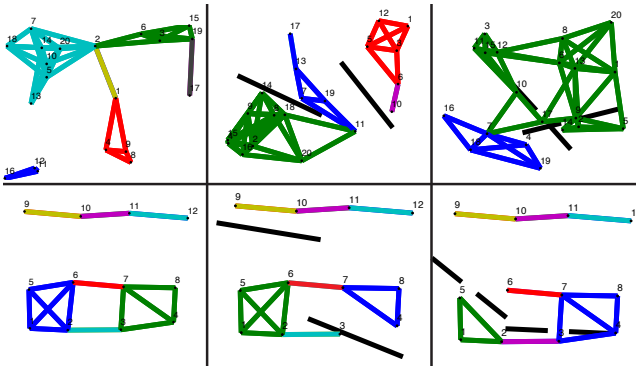

Fig. 5: We are able to identify rigidly-constrained components in embedding problems when a global coordinate frame is available. **Top row**: randomly-generated configurations of 20 nodes. **Bottom row**: a configuration of quadrotors. Each column shows a different visibility mode. **First column**: each node can sense others within 1.5m. **Second column**: two random walls block visibility in addition to a 1.5m sensor range. **Third column**: two random sets of two pillars block visibility in addition to a 1.5m sensor range.

Each rigid component's embedding is solved separately and Procrustes analysis is performed to align the reconstruction with the ground truth. We report the mean squared distances between points. In all cases, mean error measurements are very low. There are also several interesting patterns in the data. First, both the mean error and its variability tend to decrease as the visibility radius increases. This happens because with a higher-visibility radius there are more connections and our global optimization procedure is able to better remove noise by reconciling redundant constraints. Also, note that in all cases the majority of constraints are part of a triangle, and with an intermediate visibility radius this proportion reaches $80-90\%$. This supports our claim that triangles are common due to the geometric constraints of Euclidean space.

VI. DISCUSSION

We have proposed algorithms for two formulations of the angular embedding problem. When global angles are known, we have presented a novel method for identifying rigid components. When only relative bearings are known, we have given a spectral algorithm to solve the embedding problem and find a globally-optimal solution for triangular constraints. We have also extended this method to account for nodes which are transitively connected to triangular constraints. Together, these two graph setups account for many common real-world situations. Although we have not dealt with relative angle constraints that are not part of a rigid component, our algorithm can be used as an initialization for iterative algorithms that incorporate these constraints.

It's also interesting to note that solutions for the embedding problem both with and without a global coordinate system are characterized by linear constraints. This allows us to solve heterogeneous problems in which only a subset of nodes are aware of their orientation by combining all linear constraints for both types of nodes into a single linear system.

Mean reconstruction errors (mm) from relative angle constraints in a 4×4-meter area

Random configurations (20 nodes)

Noise (°)	Visibility 1.5m	2m	3m	4m	walls	pillars
$\mathcal{U}(-1,1)$	46.87 ± 133.0 mm	13.30 ± 49.16 mm	2.667 ± 0.602 mm	2.265 ± 0.384 mm	69.04 ± 255.6 mm	19.45 ± 133.6 mm
$\mathcal{N}(0, 0.5^2)$	49.50 ± 151.7 mm	10.71 ± 47.79 mm	2.385 ± 0.582 mm	1.952 ± 0.302 mm	79.59 ± 285.9 mm	7.747 ± 26.16 mm
$\mathcal{N}(0, 0.3^2)$	13.28 ± 37.45 mm	14.76 ± 113.6 mm	1.383 ± 0.312 mm	1.172 ± 0.187 mm	8.576 ± 28.97 mm	1.901 ± 1.932 mm
$\mathcal{N}(0, 0.1^2)$	15.94 ± 103.6 mm	1.382 ± 2.017 mm	0.456 ± 0.110 mm	0.379 ± 0.052 mm	10.60 ± 91.33 mm	0.802 ± 1.289 mm
Proportion triangular	0.62	0.70	0.87	0.98	0.84	0.80

Quadrotor configurations (12 nodes)

Noise (°)	Visibility 1.5m	2m	3m	4m	walls	pillars
$\mathcal{U}(-1,1)$	6.817 ± 4.177 mm	7.163 ± 9.244 mm	2.889 ± 1.099 mm	2.720 ± 0.747 mm	16.25 ± 73.45 mm	10.71 ± 53.41 mm
$\mathcal{N}(0, 0.5^2)$	5.907 ± 3.866 mm	6.095 ± 8.166 mm	2.540 ± 0.980 mm	2.337 ± 0.701 mm	20.25 ± 80.02 mm	7.949 ± 38.75 mm
$\mathcal{N}(0, 0.3^2)$	3.548 ± 2.319 mm	3.139 ± 3.413 mm	1.521 ± 0.575 mm	1.408 ± 0.403 mm	11.68 ± 58.78 mm	2.918 ± 5.136 mm
$\mathcal{N}(0, 0.1^2)$	1.164 ± 0.745 mm	1.009 ± 1.037 mm	0.504 ± 0.194 mm	0.470 ± 0.139 mm	1.793 ± 4.961 mm	1.099 ± 3.271 mm
Proportion triangular	0.66	0.81	0.97	0.99	0.86	0.85

TABLE I: Quantitative results for our algorithm with relative angular constraints. We show the mean and standard deviation of reconstruction errors (in mm) after alignment to ground truth data. We use both random configurations of nodes and configurations of actual quadrotors. Noise was added independently to each angle based on either a uniform ($\mathcal{U}$) or normal ($\mathcal{N}$) distribution. For the quadrotor configurations, 6 different formations were selected. In both cases, results were averaged over 100 trials. Errors are calculated over all constraints that were part of a trianglular-constrained subproblems and thus optimized by our method; in the last row of each section we show the proportion of all constraints that were part of triangles.

REFERENCES

[1] B. Servatius and W. Whiteley, "Constraining plane configurations in cad: Combinatorics of directions and lengths," *SIAM J. Discrete Math*, vol. 12, pp. 136–153, 1999.

[2] T. Eren, W. Whiteley, and P. Belhumeur, "A theoretical analysis of the conditions for unambiguous node localization in sensor networks," *Columbia University, Computer Science Department, Tech. Rep. CUCS-032-04*, 2004.

[3] Y. Dieudonne, O. Labbani-Igbida, and F. Petit, "Deterministic robot-network localization is hard," *IEEE Transactions on Robotics*, vol. 26, no. 2, pp. 331–339, 2010.

[4] J. Aspnes, T. Eren, D. Goldenberg, A. Morse, W. Whiteley, Y. Yang, B. Anderson, and P. Belhumeur, "A theory of network localization," *IEEE Transactions on Mobile Computing*, vol. 5, no. 12, pp. 1663–1678, 2006.

[5] G. Laman, "On graphs and rigidity of plane skeletal structures," *Journal of Engineering mathematics*, vol. 4, no. 4, pp. 331–340, 1970.

[6] J. Saxe, *Embeddability of weighted graphs in k-space is strongly NP-hard*. Carnegie-Mellon University, Dept. of Computer Science, 1980.

[7] W. Torgerson, "Multidimensional scaling: I. theory and method," *Psychometrika*, vol. 17, no. 4, pp. 401–419, 1952.

[8] F. Zhang, R. Kumar, and G. Pereira, "Necessary and sufficient conditions for localization of multiple robot platforms," *Departmental Papers (MEAM)*, p. 56, 2004.

[9] T. Eren, O. Goldenberg, W. Whiteley, Y. Yang, A. Morse, B. Anderson, and P. Belhumeur, "Rigidity, computation, and randomization in network localization," in *IEEE International Conference on Computer Communications*, vol. 4. IEEE, 2004, pp. 2673–2684.

[10] A. So and Y. Ye, "Theory of semidefinite programming for sensor network localization," *Mathematical Programming*, vol. 109, no. 2, pp. 367–384, 2007.

[11] D. Moore, J. Leonard, D. Rus, and S. Teller, "Robust distributed network localization with noisy range measurements," in *Proceedings of the 2nd international conference on Embedded networked sensor systems*. ACM, 2004, pp. 50–61.

[12] A. Howard, "Multi-robot simultaneous localization and mapping using particle filters," *The International Journal of Robotics Research*, vol. 25, no. 12, pp. 1243–1256, 2006.

[13] L. Doherty, L. El Ghaoui, *et al.*, "Convex position estimation in wireless sensor networks," in *IEEE International Conference on Computer Communications*, vol. 3. Ieee, 2001, pp. 1655–1663.

[14] J. Spletzer and C. J. Taylor, "A bounded uncertainty approach to multi-robot localization," in *IEEE/RSJ International Conference on Intelligent Robots and Systems (IROS)*, 2003, pp. 1258–1264.

[15] A. Martinelli, F. Pont, and R. Siegwart, "Multi-robot localization using relative observations," in *IEEE International Conference on Robotics and Automation*. IEEE, 2005, pp. 2797–2802.

[16] G. Piovan, I. Shames, B. Fidan, F. Bullo, and B. Anderson, "On frame and orientation localization for relative sensing networks," in *IEEE Conference on Decision and Control*. IEEE, 2008, pp. 2326–2331.

[17] F. Dellaert and A. Stroupe, "Linear 2d localization and mapping for single and multiple robot scenarios," in *IEEE International Conference on Robotics and Automation*, vol. 1. IEEE, 2002, pp. 688–694.

[18] L. Quan and T. Kanade, "Affine structure from line correspondences with uncalibrated affine cameras," *IEEE Transactions on Pattern Analysis and Machine Intelligence*, vol. 19, no. 8, pp. 834–845, 1997.

[19] N. Trawny, X. Zhou, K. Zhou, and S. Roumeliotis, "Interrobot transformations in 3-d," *IEEE Transactions on Robotics*, vol. 26, no. 2, pp. 226–243, 2010.

[20] M. Brand, M. Antone, and S. Teller, "Spectral solution of large-scale extrinsic camera calibration as a graph embedding problem," *European Conference on Computer Vision*, pp. 262–273, 2004.

[21] C. Taylor and J. Spletzer, "A bounded uncertainty approach to cooperative localization using relative bearing constraints," in *IEEE/RSJ International Conference on Intelligent Robots and Systems*. IEEE, 2007, pp. 2500–2506.

[22] Y. Zhou, "Combinatorial decomposition, generic independence and algebraic complexity of geometric constraints systems: applications in biology and engineering," Ph.D. dissertation, University of Florida, 2006.

[23] C. Lanczos, "An iteration method for the solution of the eigenvalue problem of linear differential and integral operators1," *Journal of Research of the National Bureau of Standards*, vol. 45, no. 4, 1950.

[24] A. Kushleyev, D. Mellinger, and V. Kumar, "Towards a swarm of agile micro quadrotors," in *Robotics: Science and Systems (RSS)*, 2012.